Photochemistry of $[CpMo(CO)_3]_2$ (Cp = η^5-C_5H_5) and $[Cp^*Fe(CO)_2]_2$ (Cp^* = η^5-C_5Me_5) in Supercritical CO_2: A Fast Time-Resolved Infrared Spectroscopic Study

Xue Z. Sun, Sergei M. Nikiforov,† Alain Dedieu,‡ and Michael W. George*

School of Chemistry, University of Nottingham, University Park, Nottingham NG7 2RD, U.K.

Received September 8, 2000

Fast (ns) time-resolved infrared spectroscopy has been used to follow the visible (532 nm) flash photolysis of *trans*-$[CpMo(CO)_3]_2$ (Cp = η^5-C_5H_5) in supercritical CO_2 ($scCO_2$) (35 °C, 2100 psi). The primary photoproduct observed on this time scale is the $CpMo(CO)_3$ radical, which dimerizes to form both *trans*- and *gauche*-$[CpMo(CO)_3]_2$. The dimerization of $CpMo(CO)_3$ has been monitored as a function of pressure, and the estimated rate constant is slightly below the expected diffusion-controlled limit. The rate constant ($2k_2$) decreases from 3.9×10^{10} to 9.9×10^9 M^{-1} s^{-1} as the pressure is increased from 79 to 213 bar. $CpMo(CO)_3$ displays three ν(CO) bands in $scCO_2$, compared to two ν(CO) bands in *n*-heptane solution and supercritical Xe (scXe), indicating that the radicals are interacting with CO_2. We find that *gauche*-$[CpMo(CO)_3]_2$ decays ($k_{obs} = 3 (\pm 0.5) \times 10^2$ s^{-1}) to the more stable *trans* isomer at similar rates in $scCO_2$ and *n*-heptane solution. Visible photolysis (532 nm) of $[Cp^*Fe(CO)_2]_2$ (Cp^* = η^5-C_5Me_5) in $scCO_2$ generates $Cp^*Fe(CO)_2$ radicals which dimerize ($2k_2 = 9.7$ ($\pm$0.3) M^{-1} s^{-1}) to form both *cis*-$[Cp^*Fe(CO)_2]_2$ and *trans*-$[Cp^*Fe(CO)_2]_2$. We observed no spectroscopic evidence for the interaction of $Cp^*Fe(CO)_2$ with CO_2, but the recombination of $Cp^*Fe(CO)_2$ in $scCO_2$ is lower than the expected diffusion-controlled rate calculated using the Stokes−Einstein equation, which may indicate a radical−CO_2 interaction. With increasing pressure, the rate constant for the dimerization of $Cp^*Fe(CO)_2$ radicals decreases from 3.0×10^{10} M^{-1} s^{-1} at 83 bar to 9.7×10^9 M^{-1} s^{-1} at 178 bar.

Introduction

The use of supercritical fluids as media for chemical reactions is becoming increasingly attractive.[1] This is due partially to supercritical CO_2 ($scCO_2$) being an environmentally acceptable replacement for toxic organic solvents in industrial processes.[2] In addition, the enhanced solubility of permanent gases such as H_2 in supercritical fluids has allowed the preparation and isolation of previously unknown organometallic complexes, $CpMn(CO)_2(\eta^2\text{-}H_2)$[3−5] and $CpNb(CO)_3$(ethylene).[6] A range of catalytic reactions have recently been carried out in $scCO_2$, including epoxidation,[8] hydroformylation,[9] and other C−C bond-forming reactions.[10]

Supercritical fluids are uniquely "tunable", and their physical properties, such as visocity, dielectric constant, and diffusivity, vary with density, which is a strong function of temperature and pressure.[1] There is considerable evidence to show that the local density of a supercritical fluid around a solute may be considerably greater than the bulk density.[11] Interest in the effect of the supercritical environment on reactions has also increased in recent years due to many intriguing results obtained near the critical point. There have been several investigations[12] into the effect of the supercritical environment on the reactions of organic excited states and radicals. In contrast, there have been relatively few reports on the effect of the supercritical environment on the rates of organometallic reactions. Eyring and coworkers have reported[13] very high activation volumes

* To whom correspondence should be addressed. E-mail: mike.george@nottingham.ac.uk.

† Permanent address: General Physics Institute, 38 Vavilov Street, 117942 Moscow, Russia.

‡ Laboratoire de Chemie, Quantique, UPR 139 du CNRS, Unversité Louis Pasteur, 4 rue Blaise Pascal, F 67000 Strasbourg, France.

(1) McHugh, M. A.; Krukonis, V. J. in *Supercritical Fluid Extraction* 2nd Ed.; Butterworth-Heinemann, 1994.

(2) See: *Green Chemistry Frontiers in Benign Chemical Synthesis and Processes*; Anastas, P. T., Williamson, T. C., Eds.; Oxford University Press: Oxford, U.K., 1998; Chapter 16.

(3) Howdle, S. M.; Poliakoff, M. *J. Chem. Soc., Chem. Commun.* **1989**, 1099.

(4) Banister, J. A.; Lee, P. D.; Poliakoff, M. *Organometallics* **1995**, *14*, 3876.

(5) Linehan, J. C.; Wallen, S. L.; Yonker, C. R.; Bitterwolf, T. E.; Bays, J. T. *J. Am. Chem. Soc.* **1997**, *119*, 10170.

(6) Linehan, J. C.; Yonker, C. R.; Bays, J. T.; Autrey, S. T.; Bitterwolf, T. E.; Gallagher, S. *J. Am. Chem. Soc.* **1998**, *120*, 10170.

(7) Burk, M. J.; Feng, S.; Gross, M. F.; Tumas, W. *J. Am. Chem. Soc.* **1995**, *117*, 8277.

(8) Perisi, D. R.; Morita, D. K.; Glaze, W.; Tumas, W. *Chem. Commun.* **1998**, 1015.

(9) (a) Bach, I.; Cole-Hamilton, D. J. *Chem. Commun.* **1998**, 1463. (b) Kainz, S.; Koch, D.; Wolfgang, B.; Leitner, W. *Angew. Chem., Int. Ed.* **1998**, *36*, 1628.

(10) Carroll, M. A.; Homes, A. B. *Chem. Commun.* **1998**, 1395.

(11) Kim, S.; Johnson, K. P. *AIChE J.* **1987**, *33*, 1603.

(12) (a) Kim, S.; Johnson, K. P. *Ind. Eng. Chem. Res.* **1987**, *26*, 1206. (b) Yonker, C. R.; Smith, R. D. *J. Phys. Chem.* **1988**, *92*, 2374. (c) Kajimoto, O.; Futakami, M.; Kobayashi, T.; Yamasaki, K. *J. Phys. Chem.* **1988**, *92*, 1347. (d) Brennecke, J. F.; Tomasko, D. L.; Peshkin, J.; Eckert, C. A. *Ind. Eng. Chem. Res.* **1990**, *29*, 1682. (e) Eckert, C. A.; Knutson, B. L. *Fluid Phase Equil.* **1993**, *83*, 93. (f) Carlier, C.; Randolph, T. W. *AIChE J.* **1993**, *39*, 876. (g) Wu., R.-S.; Lee, L. L.; Cochran, H. D. *Ind. Eng. Chem. Res.* **1990**, *29*, 977. (h) McGuigan, D. B.; Monson, P. A. *Fluid Phase Equil.* **1990**, *57*, 227. (i) Chialvo, A. A. *J. Phys. Chem.* **1993**, *97*, 2740. (j) Petsche, I. B.; Debenedetti, P. G. *J. Chem. Phys.* **1989**, *91*, 7075. (k) Chialvo, A. A.; Debenedetti, P. G. *Ind. Eng. Chem. Res.* **1992**, *31*, 1391. (l) O'Brien, J, A.; Randolph, T. W.; Carlier, C.; Shankar, G. *AIchE J.* **1993**, *39*, 1061.

10.1021/om000771b CCC: $20.00
Publication on Web 03/13/2001

Scheme 1

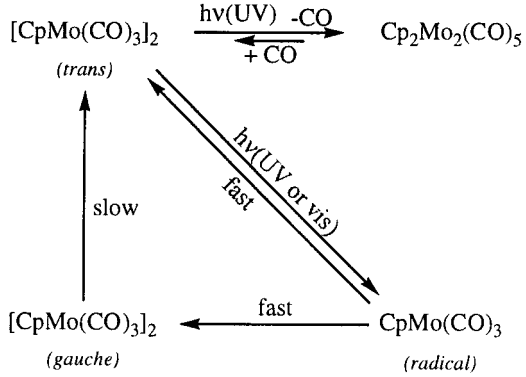

just above the critical point[13] for the ring-closure reactions of $M(CO)_5L-L$ (M = Cr, M; L−L denotes a bidentate ligand) in $scCO_2$ and supercritical ethane.

Fast time-resolved IR spectroscopy (TRIR) has proved[14] to be a powerful tool for elucidating the reactivity of organometallic radicals in conventional solvents at room temperature. We recently reported the combination of TRIR and supercritical fluids to characterize complexes such as $M(CO)_5L$ (M = Cr, Mo, W; L = Kr, Xe, CO_2),[15] $CpRe(CO)_2L$ (Cp = η^5-C_5H_5; L = Kr, Xe)[16] and $CpM(CO)_2(CO_2)$[17] (M = Mn, Re) in solution at room temperature. The lifetime of $W(CO)_5(CO_2)$ in $scCO_2$ was shown[15] to be proportional to the density of $scCO_2$. To date there have been no experimental investigations into the effect of the supercritical fluid environment on the reactivity of organometallic radicals. In this paper[18] we probe the photochemistry of *trans*-$[CpMo(CO)_3]_2$ (**1**) in supercritical CO_2. We have chosen **1** as a model to probe the reactivity of organometallic radicals in $scCO_2$, since the photochemistry of **1** has recently been investigated in *n*-heptane using TRIR.[19] This will allow us to compare directly the reactivity between conventional and supercritical fluid. Visible irradiation (532 nm) of **1** in *n*-heptane solution resulted only in the cleavage of the Mo−Mo bond to produce the $CpMo(CO)_3$ radicals, **R**. In *n*-heptane solution **R** molecules recombine at a diffusion-controlled rate to form both **1** and the unstable *gauche*-$[CpMo(CO)_3]_2$ (**4**). This is followed by slow isomerization of **4** to **1**. The photochemistry of **1** is summarized in Scheme 1.

Experimental Section

The Nottingham diode laser based TRIR apparatus has been described in detail elsewhere.[14] In these experiments two different types of TRIR instrumentation were used, both of which employed a pulsed visible source (Nd:YAG laser (Quanta-Ray GCR-12)) to initiate photochemical reactions. A step-scan FTIR interferometer (Nicolet Magna 860) or a CW IR diode laser (Mütek MDS 1100) was used to monitor the transient IR absorptions. A detailed account of the experimental apparatus for using the step-scan FTIR interferometer for time-resolved IR measurements will be the subject of a future publication.[20] Briefly, the apparatus is comprised of a commercially available step-scan FTIR spectrometer (Nicolet Magna 860), equipped with a 100 MHz 12-bit digitizer, and a 50 MHz MCT detector interfaced to a Nd:YAG laser (Spectron SL80SG). Synchronization of the Nd:YAG laser with data collection was achieved using a pulse generator (Stanford DG535).

In the experiments using IR diode lasers, the change in IR transmission at one particular frequency was measured following excitation with a Nd:YAG laser (Quanta-Ray GCR-12; 532 nm, 7 ns pulse). IR spectra were built up on a "point-by-point" basis by repeating this measurement at different infrared frequencies. The stainless steel cell used for supercritical TRIR measurements has been described previously for conventional spectroscopic monitoring.[21] CO_2 (Air products SFC Grade) was dried over molecular sieves prior to use. $[CpMo(CO)_3]_2$ (Aldrich) was used as supplied.

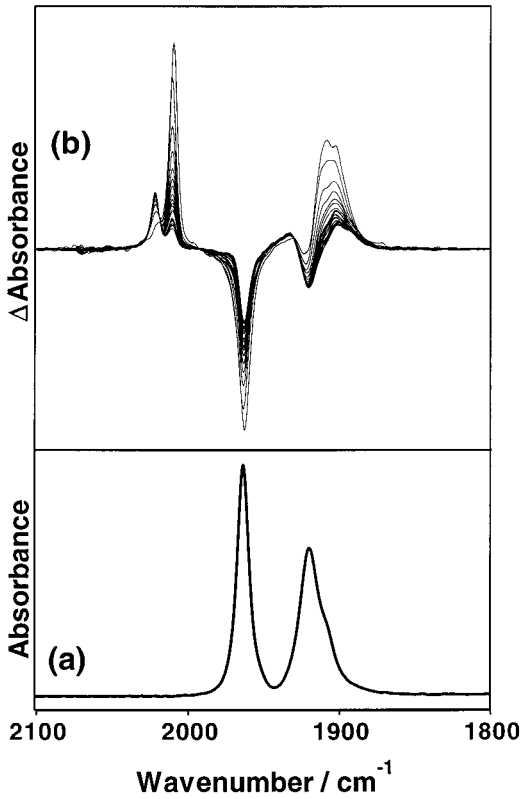

Figure 1. (a) FTIR spectrum of *trans*-$[CpMo(CO)_3]_2$ in $scCO_2$ (35 °C, 2800 psi). (b) Series of TRIR spectra (in 500 ns increments) showing the conversion $CpMo(CO)_3^{\bullet} \rightarrow$ *trans*-$[CpMo(CO)_3]_2$ + *gauche*-$[CpMo(CO)_3]_2$. All TRIR spectra shown in this figure were obtained by averaging four scans of the FTIR interferometer.

Results and Discussion

Photolysis of *trans*-$[CpMo(CO)_3]_2$ at 532 nm in $scCO_2$: Identification of $CpMo(CO)_3$ Radicals and *gauche*-$[CpMo(CO)_3]_2$ in $scCO_2$ Solution. Figure 1a shows the FTIR spectrum of **1** in $scCO_2$ (35 °C, 2100

(13) Ji, Q.; Eyring, E. M.; Eldik, R.; Johnson, K. P.; Goates, S. R.; Lee, M. L. *J. Phys. Chem.* **1995**, *99*, 13461. Ji, Q.; Lloyd, C. R.; Eyring; E. M.; Eldik, R. *J. Phys. Chem. A* **1997**, *101*, 243.

(14) George, M. W.; Poliakoff, M.; Turner, J. J. *Analyst* **1994**, *119*, 551.

(15) Sun, X. Z.; George, M. W.; Kazarian, S. G.; Nikiforov, S. M.; Poliakoff, M. *J. Am. Chem. Soc.* **1996**, *118*, 10525.

(16) Sun, X. Z.; Nikiforov, S. M.; Grills, D. C.; Poliakoff, M.; George, M. W. *J. Am. Chem. Soc.* **1997**, *119*, 7521.

(17) George, M. W.; Sun, X. Z.; Grills, D. C.; Poliakoff, M. *Stud. Surf. Sci. Catal.* **1998**, *114*, 255.

(18) We have used Brown's notation[30] throughout the text to be consistent with our previous[19] TRIR study on *trans*-$[CpMo(CO)_3]_2$.

(19) Peters, J.; George, M. W.; Turner, J. J. *Organometallics* **1995**, *14*, 1503.

(20) Sun, X. Z.; Nikiforov, X. Z.;.; George, M. W. *Appl. Spectrosc.*, submitted.

(21) Howdle, S. M.; Poliakoff, M. In *Supercritical Fluids−Fundamentals for Applications*; Kiran, E., Levelt Sengers, J. M., Eds.; Kluwer Academic: Dordrecht, The Netherlands, 1993; Vol. 273, p 527.

Table 1. Infrared Spectral Data (cm^{-1}) in the ν(CO) Region for the Species Involved in the Photochemistry of [CpMo(CO)$_3$]$_2$

species	*n*-heptane (298 K)[a]	scCO$_2$ (335 K)[b]	scXe (298 K)[b]	3-methylpentane (200 K)[c]	CO matrix (12 K)[d]
trans-[CpMo(CO)$_3$]$_2$	1964	1965	1967		
	1920	1921	1923		
	1913	1914	1915		
gauche-[CpMo(CO)$_3$]$_2$	2022	2022	2023	2021	
	ca. 1960	ca. 1965	1968	1966	
	1931	1932	1936	1930	
	1905	1904	1908	1905	
	1898	1892	1899	1895	
	1878				
CpMo(CO)$_3$	2010	2012	2012		2009
	1912	1920	1909		1908/1916[e]
		1909 (sh)			

[a] Reference 19. [b] This work. [c] Reference 30. [d] Reference 31. [e] Matrix split.

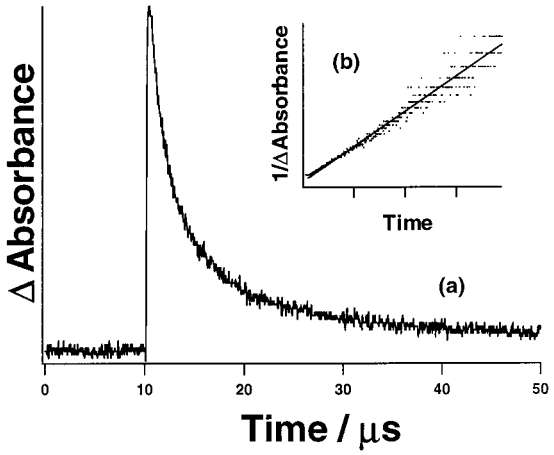

Figure 2. (a) TRIR decay trace (obtained using an IR diode laser) of CpMo(CO)$_3$ recorded at 2012 cm^{-1} following 532 nm flash photolysis of [CpMo(CO)$_3$]$_2$ in scCO$_2$ (35 °C, 2100 psi). (b) Plot of 1/Δ*A* vs time for the TRIR decay trace shown in (a).

psi). Figure 1b shows the TRIR spectrum obtained 500 ns after 532 nm excitation of this solution. It is clear from Figure 1b that visible excitation causes the depletion of **1** and the production of new IR absorption bands at 2012, 1920, and 1909 (sh) cm^{-1}. These bands decay at the same rate and hence can be assumed to derive from the same species. In comparison to the ν(CO) bands of **R** obtained from the TRIR experiments in *n*-heptane solution, together with the data obtained in low-temperature matrices, these ν(CO) bands can be assigned to the radical species **R** (see Table 1).

The TRIR spectrum obtained 20 μs after the photolysis of **1** shows that the bands of **R** decay and are replaced by new bands at 2022, 1932, 1904, and 1892 cm^{-1}, which all grow in with the same rate. The change in intensity at approximately 1968 cm^{-1} indicates the presence of another, overlapping, band which grows in as the band due to **R** decays away. This is evidenced by following computer subtraction of the parent ν(CO) absorptions. In comparison to the previous TRIR measurements in *n*-heptane and the results from low-temperature matrix isolation experiments, these bands can be assigned to **4** (see Table 1).

Determination of Radical Recombination Kinetics. Figure 2a shows a TRIR decay trace of **R** in which the change in IR absorbance at 2012 cm^{-1} is monitored as a function of time in scCO$_2$ (35 °C, 2100 psi). A plot of 1/Δ*A* vs time (Figure 2b) shows that the decay of the radical follows second-order kinetics and is consistent with a simple bimolecular recombination process (eq 1).

$$2\mathbf{R} \rightarrow \mathbf{R}_2$$

$$-\mathrm{d}[\mathbf{R}]/\mathrm{d}t = 2k_2[\mathbf{R}]^2 \qquad (1)$$

In principle, the concentration of **R** is easily determined, since the IR extinction coefficient of **1** at a particular frequency could be measured and the change in concentration of *trans*-[CpMo(CO)$_3$]$_2$ is readily monitored from the change in absorbance of **1** at that frequency. If all of **1** that is photolyzed is converted to **R**, then the concentration of **R** is obtained. *In practice*, this is difficult because there is overlap between the bands of **1** and the products (see Figure 1). This overlap is more substantial than in *n*-heptane, where previous TRIR experiments measured the decay kinetics of **R**, because the ν(CO) bands of **1** are significantly broader in scCO$_2$ (fwhm 9.4 cm^{-1}) compared to *n*-heptane (fwhm 4.8 cm^{-1}). Also, the lower frequency ν(CO) band of **R** is split in scCO$_2$ and, as a result, the IR extinction coefficient of **R** calculated from TRIR in *n*-heptane solution cannot be used. UV/visible extinction coefficients of compounds are much less sensitive to solvent compared to IR extinction coefficients. We have used the following strategy to estimate the extinction coefficient, ϵ_{2012}, and hence the rate constant for dimerization of **R** in scCO$_2$ (T = 35 °C, P = 2100 psi). We have assumed that the UV extinction coefficient of **1** will have the same value in *n*-heptane and scCO$_2$. We have then used the ratio of the absorbance in the UV at 280 nm and in the IR at 1963.6 cm^{-1} in *n*-heptane to compare with the ratio of absorbance in the UV at 280 nm and IR at 1965.1 cm^{-1} in scCO$_2$, to estimate the extinction coefficient of the parent. We performed this measurement over a range of concentrations and estimated the IR extinction coefficient of **1** at 1965 cm^{-1} (ϵ_{1965} = 1250 (±100) M^{-1} cm^{-1}). We also calculated the ϵ value by taking a small volume of known concentration of a solution of **1** in *n*-heptane and placing it in the supercritical cell. Evaporation of *n*-heptane followed by pressurization of the cell permitted the concentration of **1** to be estimated. This process was repeated for five different mixtures with a variety of concentrations. The calculated IR extinction coefficient (ϵ_{1965} = 1220 (±150) M^{-1} cm^{-1}) was consistent with the value estimated from the ratio of UV to IR bands in *n*-heptane.

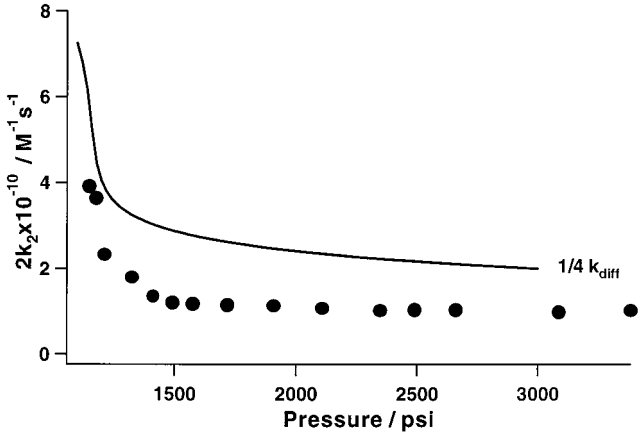

Figure 3. A plot of k_2 (●) for the decay of $CpMo(CO)_3$ in $scCO_2$ vs CO_2 pressure. These data were obtained by determining the maximum of the ν(CO) band of $CpMo(CO)_3$ as a function of pressure and then using the maximum absorption to calculate k_2. The solid line is a plot of diffusion-controlled rate constant, calculated using the Stokes−Einstein equation, vs pressure in $scCO_2$.

We have used the above result of IR extinction coefficient for the **R** in $scCO_2$ (35 °C, 2100 psi) at 2012 cm to calculate $2k_2$ ([1.2 (±0.2)] × 10^{10} M^{-1} s^{-1}). This rate is close to the diffusion rate for the recombination of two spin $^1/_2$ radicals in $scCO_2$ (see below for discussion).

Determination of Radical Recombination Kinetics as a Function of Pressure. Figure 3 shows a plot of $2k_2$ for the decay of **R** in $scCO_2$ (35 °C) measured at 2012 cm^{-1}. The calculation of $2k_2$ is complicated because we cannot use the extinction coefficient calculated above, since this interpretation requires the ν(CO) band position of the radical not to vary with pressure. Fayer and co-workers have shown that the position of the ν(CO) band of $W(CO)_6$ in $scCO_2$ varies with density of CO_2.[22] The positions of the ν(CO) bands of **1** are not constant with pressure in $scCO_2$, and changes in peak position are most marked as the pressure approaches P_c. We determined the peak position of **R** as a function of pressure and used this IR frequency to determine the radical kinetics. The ν(CO) band shape of **R** did not change significantly with pressure, and we have assumed that the extinction coefficient at the maximum of the radical band remains constant. Over all pressures we observed no evidence for the rate enhancement due to clustering of the solvent as the pressure approached P_c.[23] The second-order rate constant for the decay of **R** is consistently slightly smaller than the estimated diffusion control in $scCO_2$ using the Stokes−Einstein equation. However, Brennecke and co-workers have recently pointed out that diffusion data in $scCO_2$ may be overestimated using Stokes−Einstein based equations,[24] and they found rate constants for diffusion-controlled reactions in $scCO_2$ similar to those shown in Figure 3.

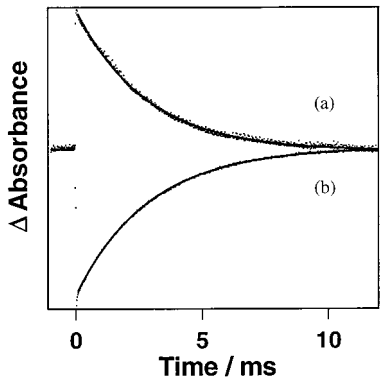

Figure 4. TRIR decay traces of (a) *gauche*-$[CpMo(CO)_3]_2$ and (b) *trans*-$[CpMo(CO)_3]_2$ recorded at 2024 and 1965 cm^{-1}, respectively, following 532 nm photolysis of *trans*-$[CpMo(CO)_3]_2$ in $scCO_2$ (35 °C, 2100 psi).

Rate of Isomerization of *gauche*- to *trans*-$[CpMo(CO)_3]_2$ (4 → 1). Following the rapid reaction of **R** to form either **1** or **4**, there is a much slower process involving the isomerization of **4** to **1**. The rate of isomerization can be measured directly by monitoring the decay of the bands at 2024 and 1965 cm^{-1}. Figure 4a shows the first-order decay of **4** at 2024 cm^{-1} in $scCO_2$ (k_{obs} = [3 (±0.5)] × 10^2 s^{-1}), which is identical with the rate of re-formation of **1** at 1965 cm^{-1} (k_{obs} = [3 (± 0.5)] × 10^2 s^{-1}) shown in Figure 4b. The rate of isomerization is very similar in $scCO_2$ and *n*-heptane (k_{obs} = 2 × 10^2 s^{-1}). The rate of isomerization remained constant in $scCO_2$ as the pressure was changed from 3000 to 1200 psi in $scCO_2$ at 35 °C.

Interaction of $CpMo(CO)_3$ Radical with CO_2. **R** was found to have three ν(CO) bands in $scCO_2$. The presence of the shoulder at 1909 cm^{-1} is more clearly shown in Figure 5, and the presence of three ν(CO) bands indicates that the local symmetry of **R** in $scCO_2$ is C_s. Only two ν(CO) bands were observed for **R** in *n*-heptane solution, indicating that the local symmetry of the CO groups is C_{3v}. However, the original TRIR measurements of **R** in *n*-heptane were obtained with lower wavenumber resolution than in the present study, and it is possible that the third band of **R** may not have been resolved.

We have repeated the TRIR measurements of **R** in *n*-heptane with higher resolution and found that **R** has indeed *only* two ν(CO) bands (Figure 5). This may indicate that CO_2 is interacting with **R** in a fashion (Lewis acid/base) similar to that observed by Kazarian et al.[25] for the interaction of $scCO_2$ with polymers. The interaction between **R** and CO_2 is supported by the IR spectrum of **R** in *n*-heptane doped with CO_2 (Figure 5). The ν(CO) bands of **R** are much narrower in *n*-heptane compared to the spectrum in $scCO_2$. In the presence of CO_2, **R** has *three* ν(CO) bands in *n*-heptane solution. It is interesting to note that the ν(CO) band pattern (frequency and intensity) of **R** in $scCO_2$ is very similar to that observed for $CpV(CO)_3(N_2)$ (Cp = η^5-C_5H_5), where the local environment is C_s, in *n*-heptane and liquid xenon solution.[26] These results strongly suggest that there is a weak Mo−CO_2 interaction, and prelimi-

(22) Urdahl, R. S.; Myers, D. J.; Rector, K. D.; Davis, P. H.; Cherayil, B. J.; Fayer, M. D. *J. Chem. Phys.* **1997**, *107*, 3747.

(23) We initially interpreted the increase of k_{obs} in terms of solvent clustering: George, M. W.; Grills, D. C.; Poliakoff, M.; Sun, X. Z. *Proceedings of TRVSVII*; Dyer, R. B., Martinez, M. A. D., Shreve, A., Woodruff, W. H., Eds.; Los Alamos National Laboratory, 1995, p 699.

(24) Zhang, J.; Roek, D. P.; Chateauneuf, J. E.; Brennecke, J. F. *J. Am. Chem. Soc.* **1997**, *119*, 9980.

(25) Kazarian, S. G.; Vincent, M. F.; Bright, F. V.; Liotta, C. L.; Eckert, C. A. *J. Am. Chem. Soc.* **1996**, *118*, 1729.

(26) Haward, M. T.; George, M. W.; Howdle, S. M.; Poliakoff, M. *J. Chem. Soc., Chem. Commun.* **1990**, 913.

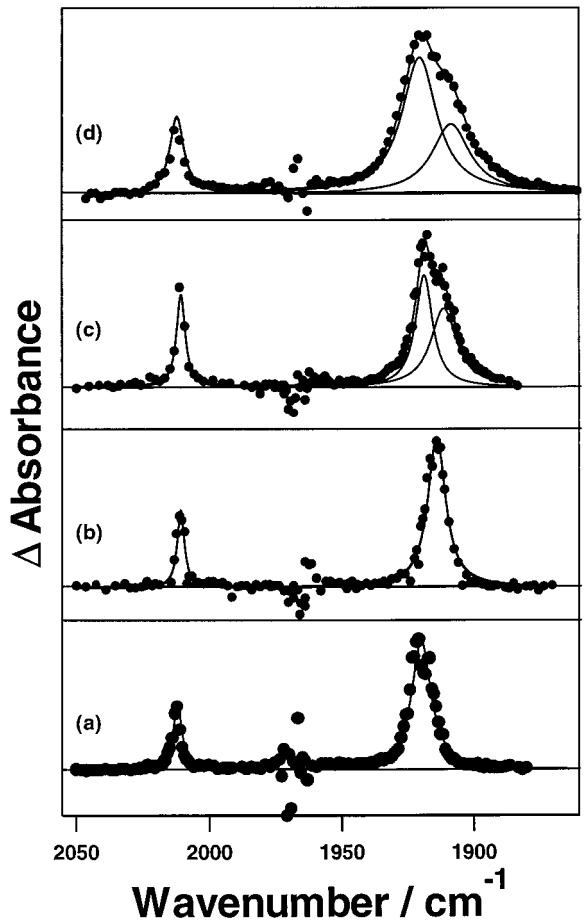

Figure 5. IR spectra of $CpMo(CO)_3$ radical produced by scaled subtraction of the FTIR spectrum of *trans*-$[CpMo(CO)_3]_2$ from the TRIR spectrum obtained 500 ns following 532 nm irradiation of *trans*-$[CpMo(CO)_3]_2$ in (a) scXe, (b) *n*-heptane, (c) *n*-heptane doped with CO_2 (100 psi), and (d) $scCO_2$ (35 °C, 2100 psi). The solid points (●) indicate data calculated by a scaled subtraction of the FTIR spectrum of $[CpMo(CO)_3]_2$ in $scCO_2$ from the TRIR spectrum obtained using the IR diode laser spectrometer. The solid line through each spectrum represents a multi-Lorentzian fit to these data.

nary[27] ab initio calculations favor a C_s structure in which the CO_2 molecule interacts weakly with the molybdenum center through one of its oxygen atoms. During these measurements great care was taken in removing possible impurities from the CO_2, e.g. H_2O.

Photochemistry of $[Cp^*Fe(CO)_2]_2$ in $scCO_2$. We have investigated[28] the reactivity of other organometallic radicals in $scCO_2$ by examining the photochemistry of $[Cp^*Fe(CO)_2]_2$. The room-temperature photochemistry of $[Cp^*Fe(CO)_2]_2$ ($Cp^* = \eta^5$-C_5Me_5) in alkane solvents has been studied[29] extensively using a variety of techniques, including TRIR. $[Cp^*Fe(CO)_2]_2$ exists in nonpolar solution exclusively as the *trans* isomer. Visible photolysis of *trans*-$[Cp^*Fe(CO)_2]_2$ results in cleavage of the Fe−Fe bond and production of $Cp^*Fe(CO)_2$ radicals, which recombine to form both *cis*- and *trans*-$[Cp^*Fe(CO)_2]_2$. *cis*-$[Cp^*Fe(CO)_2]_2$ slowly isomerizes to *trans*-$[Cp^*Fe(CO)_2]_2$. Figure 6 shows the infrared spectra of the $Cp^*Fe(CO)_2$ radical obtained in $scCO_2$ and *n*-heptane following visible irradiation (532 nm) of *trans*-$[Cp^*Fe(CO)_2]_2$. It is clear that the parent bands are bleached and two new bands are produced at 1982 and 1911 cm^{-1}. These two new absorptions can be assigned to the $Cp^*Fe(CO)_2$ radical by comparison with previous TRIR results in cyclohexane (see Table 2). Similar results are obtained in *n*-heptane solution. $Cp^*Fe(CO)_2$ decays to form *cis*- and *trans*-$[Cp^*Fe(CO)_2]_2$ radicals, and then the *cis* isomer slowly isomerizes to the more stable *trans* isomer (not shown). We have estimated, using the method described above for **R**, the second-order rate constant ($2k_2 = [9.7\ (\pm 0.3)] \times 10^9\ M^{-1}\ s^{-1}$) for recombination of $Cp^*Fe(CO)_2$ in $scCO_2$ (35 °C, 2250 psi). The determination of the $2k_2$ value of $Cp^*Fe(CO)_2$

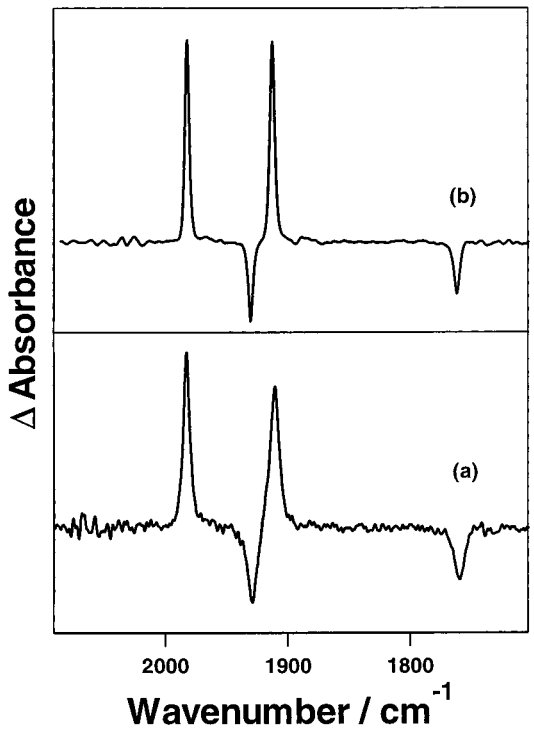

Figure 6. TRIR spectra obtained 500 ns after photolysis (532 nm) of $[Cp^*Fe(CO)_2]_2$ in (a) $scCO_2$ (35 °C, 2250 psi) and (b) *n*-heptane.

Table 2. Infrared Spectral Data (cm^{-1}) in the ν(CO) Region for the Species Involved in the Photochemistry of $[Cp^*Fe(CO)_2]_2$

species	$scCO_2$ 308 K[a]	*n*-heptane 298 K[a]	cyclohexane 298 K[b]	MCH[c] 298 K	MCH[c] 77 K
trans-$[Cp^*Fe(CO)_2]_2$	1930	1931	1928	1933	1926
	1761	1762	1765	1765	1754
cis-$[Cp^*Fe(CO)_2]_2$	1981	1982	1981		
	1755	1748	1756		
$Cp^*Fe(CO)_2$	1982	1983	1984		2009
	1911	1913	1915		1915.5
$Cp^*_2Fe_2(CO)_3$			1790		1785

[a] This work. [b] Reference 29. [c] Reference 32. MCH = methylcyclohexane.

(27) These calculations were performed out at the MP2 level, with a basis set of valence double-ζ quality and including polarization functions on the Pd atom and the CO_2 atoms. At this level of calculation an optimized Mo···O distance of 3.08 Å is obtained. Additional calculations at a higher level of theory are presently being carried out. Dedieu, A.; George, M. W. To be submitted for publication.

(28) Preliminary investigation into the photochemistry of $[Cp^*Fe(CO)_2]_2$ has been reported in a conference proceeding (Poliakoff, M.; Howdle, S. M.; Jobling, M.; George, M. W. *Proc. 2nd Int. Conf. Supercritical Fluids, Boston* **1991**, 191.

(29) Moore, B. D.; Poliakoff, M.; Turner, J. J. *J. Am. Chem. Soc.* **1986**, *108*, 1819.

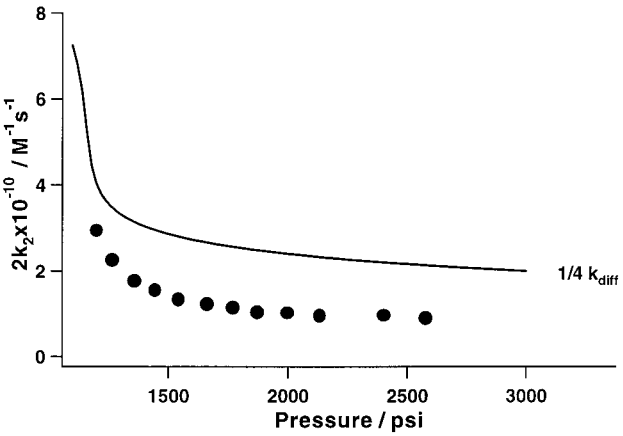

Figure 7. Plot of k_2 (●) for the decay of $CpFe(CO)_2$ in $scCO_2$ vs CO_2 pressure. These data were obtained by determining the maximum of the ν(CO) band of $CpFe(CO)_2$ as a function of pressure and then using the maximum absorption to calculate k_2. The solid line is a plot of the diffusion-controlled rate constant, calculated using the Stokes−Einstein equation, vs pressure in $scCO_2$.

as a function of pressure shows that, similar to $CpMo(CO)_3$, $2k_2$ is slightly smaller than the diffusion-controlled rate in $scCO_2$ estimated using the Stokes−Einstein equation (Figure 7).

Conclusions

We have characterized the $CpMo(CO)_3$ radical in $scCO_2$ at 35 °C and determined the kinetics of recombination of the radical and *gauche* to *trans* isomerization of $[CpMo(CO)_3]_2$. The recombination of $CpMo(CO)_3$ radicals occurs slightly below the expected diffusion-controlled rate in $scCO_2$ at all the pressures we monitored. With increasing pressure the rate constant decreases from 3.9×10^{10} M^{-1} s^{-1} at 79 bar to 9.9×10^9 M^{-1} s^{-1} at 213 bar. The splitting of the ν(CO) bands of $CpMo(CO)_3$ in $scCO_2$ indicates that the radicals form a weak complex with CO_2. The isomerization of *gauche*-$[CpMo(CO)_3]_2$ to *trans*-$[CpMo(CO)_3]_2$ occurs at a similar rate in $scCO_2$ and *n*-heptane solution. Visible photolysis of *trans*-$[Cp^*Fe(CO)_2]_2$ in $scCO_2$ generates $Cp^*Fe(CO)_2$ radicals which dimerize ($k_2 = 9.7$ ($\pm$0.3) M^{-1} s^{-1}) to form both *cis*-$[Cp^*Fe(CO)_2]_2$ and *trans*-$[Cp^*Fe(CO)_2]_2$. We find no spectroscopic evidence for the interaction of $Cp^*Fe(CO)_2$ with CO_2. However, the recombination of $Cp^*Fe(CO)_2$ in $scCO_2$ is lower than the expected diffusion-controlled rate calculated using the Stokes−Einstein equation, which may indicate a radical−CO_2 interaction. With increasing pressure the rate constant for dimerization of $Cp^*Fe(CO)_2$ decreases from 3.0×10^{10} M^{-1} s^{-1} at 83 bar to 9.7×10^9 M^{-1} s^{-1} at 178 bar. Previous work has suggested[12] that organic radicals show enhanced rates of reaction in $scCO_2$ near T_c. Our results on $CpMo(CO)_3$ and $Cp^*Fe(CO)_2$ suggest that metal-centered radicals do not necessarily display similar enhancement because of the interaction of with the CO_2 solvent. Furthermore, CO_2 can have can a number[33] of different coordination modes to transition-metal centers, including η^2(CO)-, η^1(O)-, and η^1(C)-coordinated CO_2. It is possible that other coordination modes (e.g., η^1(*C*)-CO_2) may have binding to reactive species that is stronger than the effects observed in this paper. There is clearly much to learn about the reactivity of organometallic complexes in supercritical fluids, and it is likely that TRIR will be increasingly useful for this purpose.

Acknowledgment. We are grateful to Professors W. Leitner, M. Poliakoff, and J. J. Turner for helpful discussions. We thank Mr. M. Guyler and Mr. K. Stanley for their assistance. We thank the Royal Society (visit of S.M.N.), EU-COST, EPSRC, and Nicolet Instruments Ltd for financial support. We are particularly grateful to the EPSRC Lasers for Science Facility Laser Loan Pool for the loan of the Spectron Nd:YAG laser.

OM000771B

(30) Knorr, J. R.; Brown, T. L. *J. Am. Chem. Soc.* **1993**, *115*, 4087.
(31) Mahmoud, K. A.; Rest, A. J.; Alt, H. G. *J. Organomet. Chem.* **1983**, *246*, C37.
(32) Hepp, A. F.; Blaha, J. P.; Lewis, C.; Wrighton, M. S. *Organometallics* **1984**, *3*, 174.
(33) Gibson, D. H. *Chem. Rev.* **1996**, *96*, 2063.